Microstructural properties and formation mechanisms of GaN nanorods grown on Al_2O_3 (0001) substrates

Kyu Hyung Lee and Jeong Yong Lee
Department of Materials Science and Engineering, Korea Advanced Institute of Science and Technology (KAIST), Daejeon 305-701, Korea

Young Hae Kwon and Tae Won Kang
Quantum Functional Semiconductor Research Center, Dongguk University, Seoul 100-715, Korea

Dong Hun Kim, Dea Uk Lee, and Tae Whan Kim[a)]
Advanced Semiconductor Research Center, Division of Electronics and Computer Engineering, Hanyang University, Seoul 133-791, Korea

(Received 10 February 2009; accepted 7 April 2009)

X-ray diffraction patterns, scanning electron microscopy images, and transmission electron microscopy images showed that one-dimensional GaN nanorods with [0001]-oriented single-crystalline wurtzite structures were grown on Al_2O_3 (0001) substrates by hydride vapor-phase epitaxy without a catalyst. The tip morphology of the GaN nanorods became flat with increasing temperature difference between the gas mixing and the substrate zones. The gas mixing temperature significantly affected the formation of the nanorods, and the substrate temperature influenced the morphology and the strain of the GaN nanorods near the GaN/Al_2O_3 heterointerface. The strain and the stress existing in the GaN layer near the heterointerface were decreased with increasing growth rate. The formation mechanisms of the GaN nanorods grown on the Al_2O_3 (0001) substrates are described on the basis of the experimental results.

I. INTRODUCTION

GaN-based materials have attracted a great deal of interest for optoelectronic devices operating in the visible-ultraviolet region of the spectrum[1–3] due to their unique properties of direct and wide band gaps, large exciton binding energies, excellent chemical stabilities, and high temperature stabilities.[4–7] Because bulk GaN substrates are not available yet, GaN materials are typically grown on heterosubstrates, such as c-Al_2O_3, 6H-SiC, and Si (111) substrates. It is not easy to obtain high-quality GaN materials because of the large difference in the lattice mismatch and the thermal expansion coefficient between the GaN layer and the foreign substrate. Many studies have been carried out to obtain high-quality GaN materials over the last several years.[8,9] Among several methods for achieving a high-quality GaN, the most desirable way is the formation of single crystal GaN materials with one-dimensional (1D) nanostructures, such as nanowires and nanorods.[10] One-dimensional nanostructural materials have become particularly attractive because of their potential applications in next-generation electronic and optoelectronic nanodevices operating at relatively low power consumption.[11–14]

Hydride vapor-phase epitaxy (HVPE) is a useful growth technique for growing thick GaN layers with high deposition rate and at a relatively low cost. Several growth techniques, such as metal organic chemical vapor deposition and molecular beam epitaxy,[15,16] have been extensively used to grow high-quality 1D GaN single-crystalline nanostructures. However, the HVPE method is relatively little used to grow 1D GaN nanostructures due to the inherent difficulties of the precise precursor control.[17,18] Growth parameters such as the growth temperature, the Ga/N flow rate, and the substrate significantly affect the morphologies of the GaN nanostructures. However, relatively few studies on the effect of growth temperature on the morphologies and structures of the 1D GaN nanostructures grown on Al_2O_3 (0001) substrates by HVPE without a catalyst have been performed. Furthermore, studies concerning the formation processes of the GaN nanorods grown on Al_2O_3 (0001) substrates have not yet been performed.

This paper reports the microstructural properties and formation mechanisms of the GaN nanorods grown on Al_2O_3 (0001) substrates by HVPE without a catalyst. X-ray diffraction (XRD), scanning electron microscopy (SEM), and transmission electron microscopy (TEM) measurements were carried out to characterize the morphologies of the GaN nanorods grown on Al_2O_3 (0001) substrates. High-resolution TEM (HRTEM) measurements

a)Address all correspondence to this author.
e-mail: twk@hanyang.ac.kr
DOI: 10.1557/JMR.2009.0298

 © 2009 Materials Research Society

were performed to analyze the strain and microstructures of the GaN nanorods. The formation mechanisms of the GaN nanorods on the Al_2O_3 (0001) substrates are described on the experimental results.

II. EXPERIMENTAL DETAILS

The growth of GaN nanorods without a catalyst was performed in an improved-designed HVPE reactor.[19] The Al_2O_3 (0001) substrates were degreased in trichloroethylene (TCE), rinsed in deionized water, etched in a mixture of HF and H_2O (1:1) at 27 °C for 5 min, and rinsed in TCE again. After the Al_2O_3 (0001) wafers had been cleaned chemically, they were mounted onto a susceptor in the reaction chamber. The HVPE chamber was divided into three reaction zones. The Ga metal source was placed at the first zone of the chamber, and the HCl reaction gas and the N_2 carrier gas were supplied by using the inlet to the chamber. The HCl reaction gas and the molten Ga source were reacted and converted into gallium chloride (GaCl) with a gas phase at the first zone in this system.[20]

$$Ga_l + HCl_g \leftrightarrow GaCl_g + \frac{1}{2}H_{2g} \quad . \qquad (1)$$

The converted GaCl gas was transported to the inner chamber by using the N_2 carrier gas and was intermixed with an NH_3 gas supplied by using another inlet in the second zone. Then, after the mixed gas was transported to the Al_2O_3 (0001) substrate at the third zone, the substrate temperature was rapidly decreased and GaN began to grow on the Al_2O_3 substrate.[20]

$$GaCl_g + NH_{3g} \leftrightarrow GaN + HCl_g + H_{2g} \quad . \qquad (2)$$

The reaction temperature in the first zone, the gas mixing temperature in the second zone, and the substrate temperature in the third zone are denoted by T_1, T_2, and T_3, respectively. When the mixed gases were supersaturated due to the decrease in the temperature of the third zone, the nucleation process of GaN nanorods started to occur on the surface of the Al_2O_3 (0001) substrate. The flow rates of the samples were identical, and their gas flow rates during the growth process were maintained at the same values. The growth conditions of the samples are summarized in Table I.

TABLE I. Growth conditions of the GaN nanorods grown on Al_2O_3 (0001) substrates.

Sample condition	A	B	C	D
T_1 (°C)	850	850	850	850
T_2 (°C)	950	950	950	920
T_3 (°C)	660	670	640	660
HCl (sccm)	40	40	40	40
NH_3 (slm)	3	3	3	3
N_2 (slm)	1	1	1	1

The XRD measurements were performed by using a Rigaku D/MAX-RC diffractometer with Cu K_α radiation (The Woodlands, TX). SEM measurements were carried out using a FEI XL 30 system (Hillsboro, OR). TEM measurements were performed by a JEOL JEM-3010 transmission electron microscope operating at 300 kV (Tokyo, Japan). The samples for the cross-sectional TEM measurements were mechanically polished to a thickness of approximately 10 μm and then ion milled at 3.5 kV using Ar^+ ions.

III. RESULTS AND DISCUSSION

Figure 1 shows the XRD patterns of GaN nanorods grown on Al_2O_3 (0001) substrates at different growth temperatures. The strong (0002) and (0004) diffraction peaks corresponding to wurtzite GaN nanorods, together with a (0006) diffraction peak related to the Al_2O_3 (0001) substrate are clearly observed in Fig. 1. While only (0002) and (0004) diffraction peaks are dominantly observed in the XRD patterns of GaN nanorods for samples A, B, and D, the small intensity peak around 36.8° corresponding to the $(10\bar{1}1)$ plane together with dominant (0002) and (0004) diffraction peaks corresponding to the GaN nanorods is shown for sample C. GaN (0002) and (0004) peaks with a strong intensity indicate that the GaN nanorods are vertically well-aligned normal to the Al_2O_3 (0001) substrate. The appearance of the $(10\bar{1}1)$ diffraction peak for sample C is attributed to the atomic disorder during the initial formation stage due to a relatively lower substrate temperature of 640 °C. The appearance of the small XRD diffraction peak corresponding to the $(10\bar{1}1)$ plane is attributed to the relatively higher degree of supersaturation due to the temperature difference between T_2 and T_3. Because the lower substrate temperature and the higher degree of supersaturation lead to the low surface diffusion and the fast growth rate, the small quantity of the GaN layer with a $(10\bar{1}1)$ plane parallel to the Al_2O_3

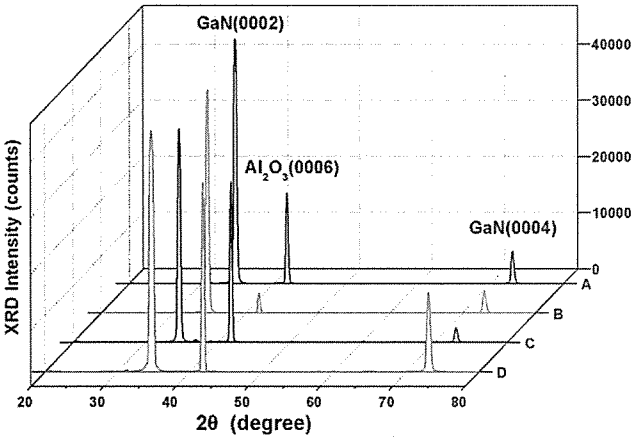

FIG. 1. X-ray diffraction patterns of the GaN nanorods grown on Al_2O_3 (0001) substrates.

(0001) substrate is formed near the GaN/Al_2O_3 hetero-interface.[21]

Figure 2 shows the cross-sectional SEM images of GaN nanorods grown on the Al_2O_3 (0001) substrate at different growth temperatures. The SEM images reveal that the morphologies of the GaN nanorods are significantly modulated by the changing gas-mixing and substrate temperatures. The heights of the GaN nanorods grown on the Al_2O_3 (0001) substrates at the same growth time for samples A, B, C, and D are approximately 1850, 2500, 1800, and 1600 nm, respectively, as shown in Fig. 2. The typical diameters of GaN nanorods for samples A, B, and C are 200, 300, and 300 nm, respectively, as shown in Fig. 2. While GaN products for samples A, B, and C have nanorod shapes, that for sample D has a thin-film shape. Because T_2 (920 °C) of sample D is lower than those of other samples, the temperature difference between T_2 and T_3 of sample D is smaller than those of other samples. The low T_2 and the small degree of the supersaturation due to the small temperature difference lead the GaN layer to form the two-dimensional (2D) thin film instead of the 1D nanorods. The morphologies of GaN nanorods are significantly affected by the substrate temperature (T_3). The tip diameter of the GaN nanorods is tapered to a point with decreasing temperature difference between T_2 and T_3, or the degree of supersaturation. The temperature differences between T_2 and T_3 for samples A, B, and C are 290, 280, and 310 °C, respectively. Because the supply amount of the Ga source is determined from the temperature difference, the growth rates of the lateral direction along the [01$\bar{1}$0] direction and of the vertical direction along the [0001] direction of GaN materials are enhanced with increasing temperature difference. While GaN nanorods for sample C have rod-like morphologies due to the large degree of supersaturation, those for sample B have needle-like shapes.

Figure 3 shows bright-field TEM (BFTEM) images of the GaN nanorods grown on the Al_2O_3 (0001) substrate at different growth temperatures. The morphology and the size of the GaN nanorods shown in the BFTEM images of Fig. 3 are in reasonable agreement with those of the SEM images shown in Fig. 2. A selected-area electron diffraction (SAED) pattern demonstrates that the growth direction of the GaN nanorods is along the *c*-axis, as shown in the inset of Fig. 3(a). The SAED pattern indicates that the orientational relationships between the Al_2O_3 substrate and the GaN nanorods are $(0001)_{GaN} \parallel (0001)_{Al_2O_3}$ and $[01\bar{1}0]_{GaN} \parallel [11\bar{2}0]_{Al_2O_3}$. The streaked diffraction spots for the GaN nanorods in the SAED pattern display that the shape of GaN nanorods are slightly tilted along the [0001] growth direction. The surface region for sample D consists of a lot of small hillocks, as shown in Fig. 3(d).

Figure 4 shows HRTEM images of the GaN nanorods grown on the Al_2O_3 (0001) substrate at different growth temperatures. The HRTEM images taken along the [2$\bar{1}\bar{1}$0] zone axis show that the facets of the GaN nanorods are significantly affected by T_2 and T_3, as shown in Fig. 4. The angles between the basal (0001) plane and the facet plane for samples A, B, C, and D are approximately 72, 80, 61, and 31°, respectively, as shown in Fig. 4. The

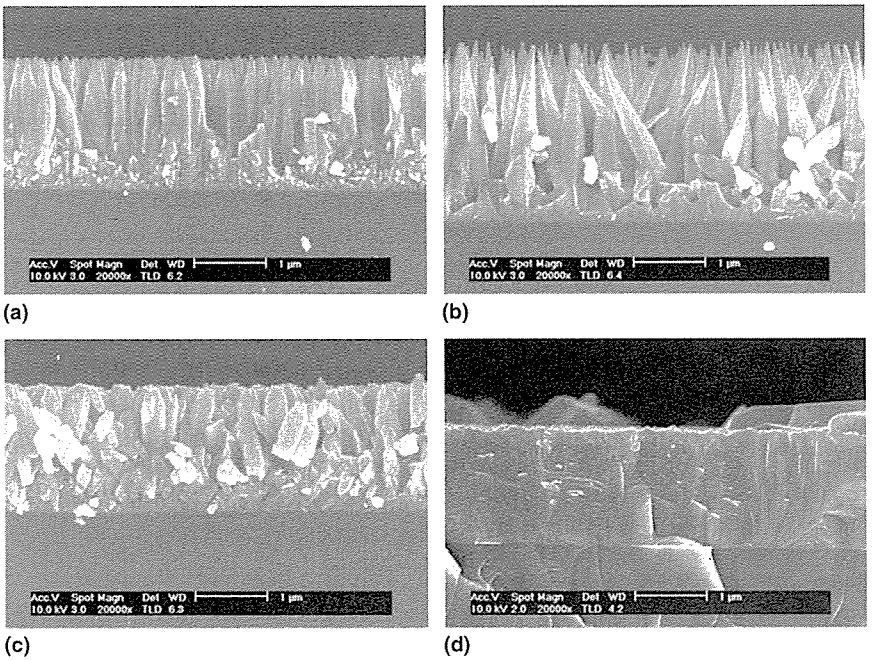

FIG. 2. Cross-sectional scanning-electron-microscopy images of GaN nanorods grown on Al_2O_3 (0001) substrates for samples (a) A, (b) B, (c) C, and (d) D.

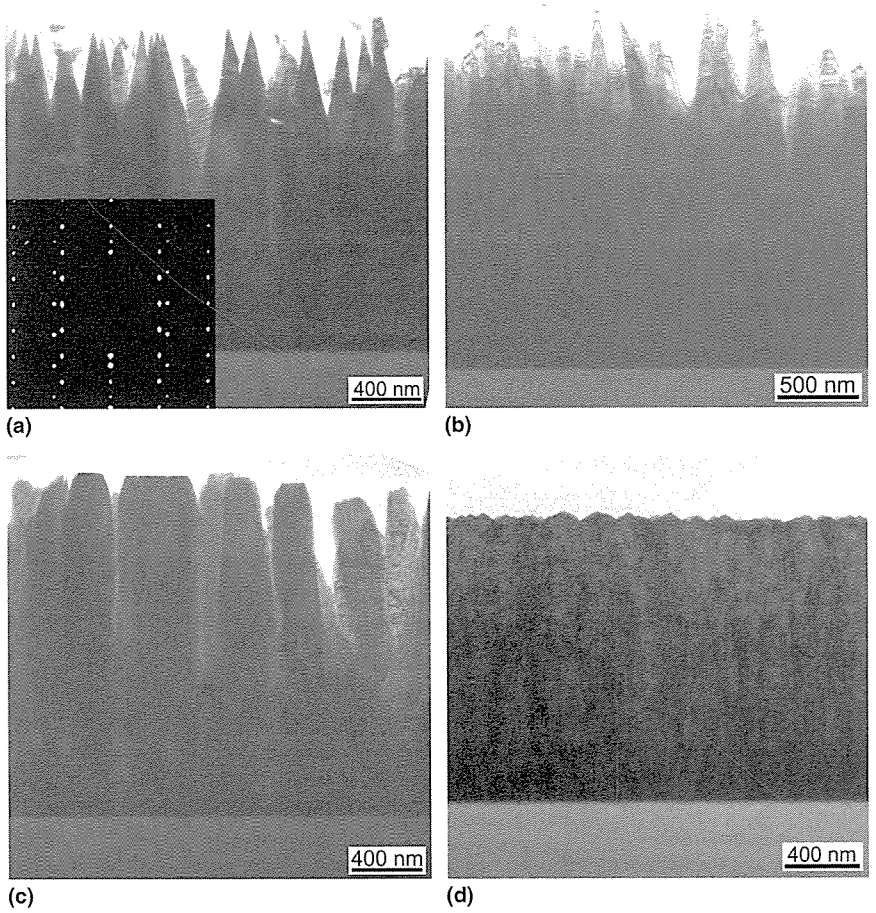

FIG. 3. Bright-field transmission electron microscopy images taken along the $[2\bar{1}\bar{1}0]$ zone axis of the GaN nanorods grown on Al_2O_3 (0001) substrates for samples (a) A, (b) B, (c) C, and (d) D. The inset of (a) indicates the selected area electron diffraction pattern of the GaN nanorods and Al_2O_3 substrate.

descendant order of the temperature difference among the nanorod-shaped samples is samples C (310 °C), A (290 °C), and B (280 °C). The inclined angle between the basal plane and the facet plane is decreased with increasing temperature difference, or the degree of the supersaturation, which originates from the increase of the lateral growth rate due to the increased supply of the Ga source. GaN products grown on the Al_2O_3 substrates have a wurtzite single crystalline structure, which is in reasonable agreement with the XRD data, and they contain some stacking faults.

The strain and stress of the GaN layer near the interfacial region between the GaN layer and the Al_2O_3 substrate are analyzed on the basis of the HRTEM images. Figure 5 shows the HRTEM images of the interfacial region for samples A and D. The interplanar spacing distances between the $(01\bar{1}0)$ and the (0001) planes of the GaN layers for samples A and B are determined to analyze the strain and stress existing in the GaN layers. The measured interplanar spacing distances of $(01\bar{1}0)$ planes for samples A and D are approximately 2.736 and 2.718 nm, respectively, and the corresponding values of the (0001) planes are 5.20 and 5.214 nm, respectively, as shown in Figs. 5(a) and 5(b). The out-of-plane (ε_c) and the in-plane strain (ε_a) components of the GaN layer are given by[22]

$$\varepsilon_c = \frac{c_r - c_0}{c_0}, \varepsilon_a = \frac{a_r - a_0}{a_0} \quad , \tag{3}$$

where c_0 and c_r are the unstrained and real (strained) c-lattice parameters, respectively, and a_0 and a_r are the unstrained and strained a-lattice parameters, respectively. The measured out-of-plane and in-plane strain components of the GaN layer for sample A are 2.70×10^{-3} and -9.41×10^{-3}, respectively, and those of the GaN layer for sample D are 5.40×10^{-3} and -1.59×10^{-2}, respectively. The in-plane biaxial stress (σ_f) of the GaN layer obeys the following equation[22]:

$$\sigma_f = M_f \varepsilon_a^{(b)} \quad , \tag{4}$$

where $M_f = c_{11} + c_{12} - 2\frac{c_{13}^2}{c_{33}}$, $\varepsilon_a^{(b)}$ is the biaxial strain in the a-direction, M_f is the biaxial elastic modulus for a material with a hexagonal structure strained about the

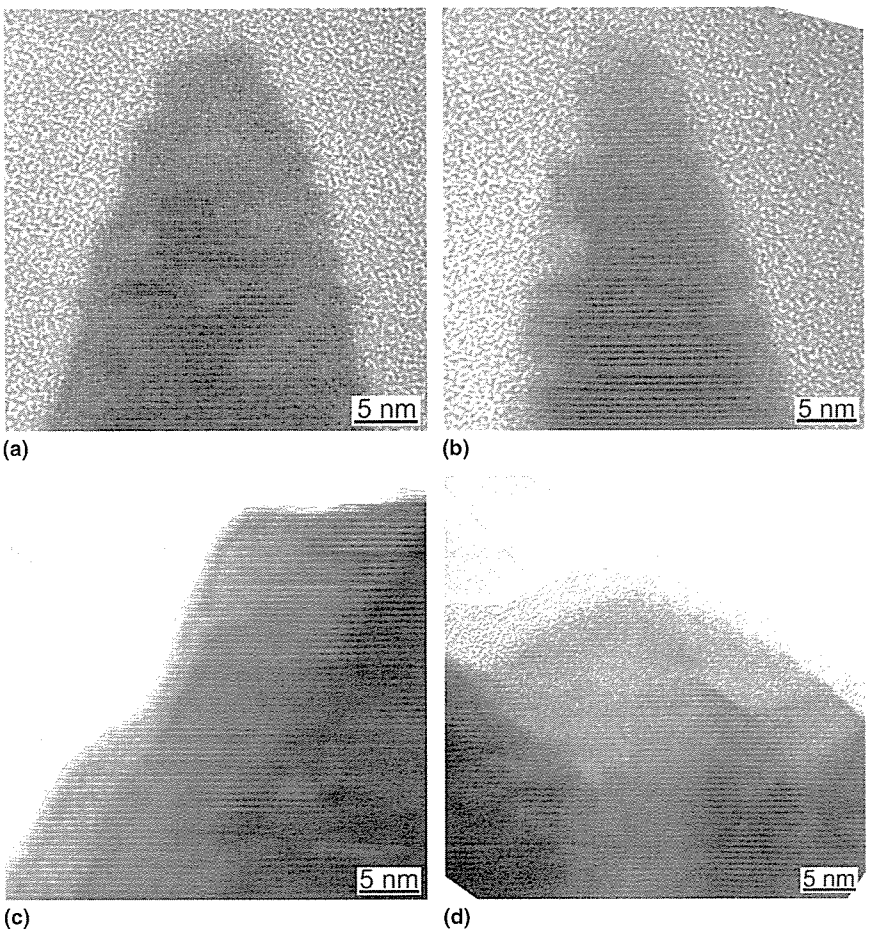

FIG. 4. High-resolution transmission electron microscopy images taken along the $[2\bar{1}\bar{1}0]$ zone axis of the GaN nanorods grown on Al_2O_3 (0001) substrates for samples (a) A, (b) B, (c) C, and (d) D.

[0001] crystallographic direction, and c_{ij} are the elastic constants of GaN. The in-plane biaxial stresses of the GaN layers for samples A and D are –3.78 and –6.66 GPa, respectively. This result indicates that the compressive stress exists in the GaN layer. The magnitude of the strain and the stress existing in the GaN layer near the heterointerface is strongly correlated to the growth rate, and the strain of the GaN layer is decreased with increasing growth rate. The GaN molecules deposited on the Al_2O_3 substrate at a slow growth rate have a diffusion time, resulting in the decrease of the lattice mismatch. However, when the growth rate is fast, the stacking quantity of GaN molecules increases, and the GaN layer has its unique lattice spacing rather than the strained spacing. The lattice mismatch between the unstrained GaN layer and the Al_2O_3 substrate is approximately 16%, and one misfit dislocation (MD) per 7.2 Al_2O_3 $(11\bar{2}0)$ planes exists. Figures 5(c) and 5(d) show the inverse fast Fourier transform (FFT) image of the interfacial region between the GaN layer and the Al_2O_3 substrate. The inverse FFT images are only obtained for the reflections of the $(11\bar{2}0)$ and $(\bar{1}\bar{1}20)$ Al_2O_3 substrate and the $(01\bar{1}0)$ and $(0\bar{1}10)$ GaN layer to clarify the MDs. The arrows indicate the MDs, or extra half planes, as shown in Figs. 5(c) and 5(d). While one MD per 7.7 Al_2O_3 $(11\bar{2}0)$ planes of sample A exists in the GaN layer, nearly one MD per eight Al_2O_3 $(11\bar{2}0)$ planes of sample D exists in the GaN layer.

Figure 6 shows schematic illustrations of the formation process of the GaN nanorods on the Al_2O_3 substrates. As mentioned above, the temperature difference between the T_2 and the T_3, or the supply amount of the GaN molecules, determines the morphologies of rod-like or needle-like nanorods. GaN molecules are transported and adsorbed on the surface of the Al_2O_3 substrate during the initial growth process, as shown in Fig. 6(a). Adsorbed GaN molecules diffuse and coalesce with neighboring GaN molecules, resulting in the creation of small islands acting as seeds for the formation of GaN nanorods, as shown in Fig. 6(b). The size of the islands formed at initial growth stage increases continuously with the addition of molecules and the coalescence of adjacent small islands, as shown in Fig. 6(c). Because the c-axis of the GaN molecules is typically the fastest

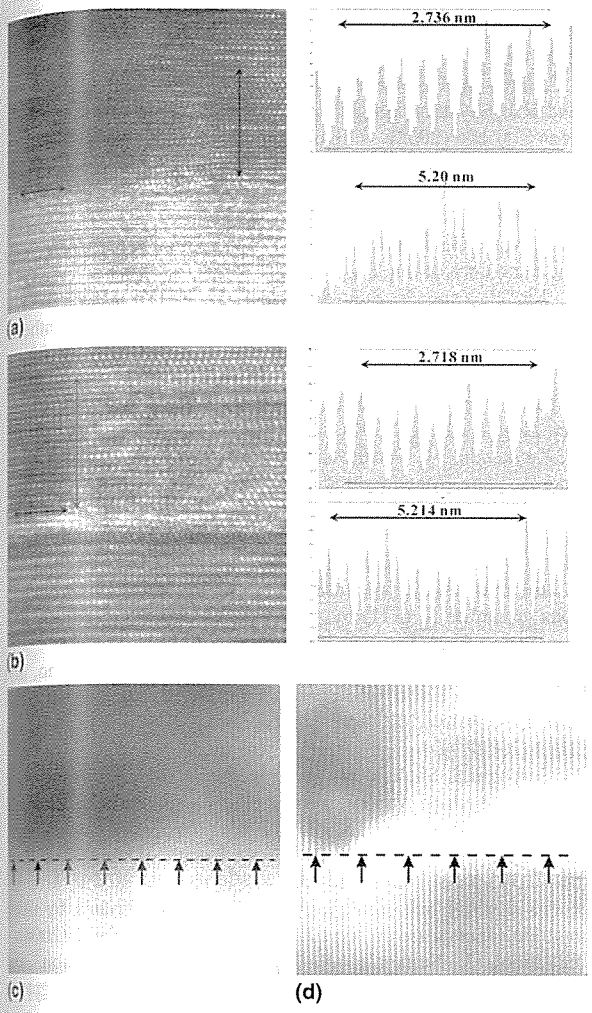

FIG. 5. High-resolution transmission electron microscopy images and interplanar spacings of the interfacial region between the GaN/Al_2O_3 heterostructure for samples (a) A and (b) D and inverse fast-Fourier transformed images of samples (c) A and (d) D. The arrows in (c) and (d) indicate the misfit dislocations.

growth direction of GaN materials, the adsorbed GaN molecules are preferentially grown along the [0001] direction. The diffusion of GaN molecules toward the tip on side facets and the direct attachment of GaN molecules at the tip of the nanorods at an initial stage significantly affect the formation process of nanorods.[23] However, the effect of direct impingement at the tip of the nanorods gradually increases. When the supply amount of GaN molecules is small, the GaN nanorods are preferentially formed along the [0001] growth direction, resulting in the formation of GaN nanorods with a needle-like shape, as shown in Fig. 6(d). When the supply amount of the sources is sufficient, the lateral growth rate of the GaN nanorods along the <01$\bar{1}$0> direction by the adatom diffusion and the vertical growth rate along the [0001] direction are increased, resulting in the formation of GaN nanorods with a rod-like shape, as shown in Fig. 6(e). While the GaN nanorods with a

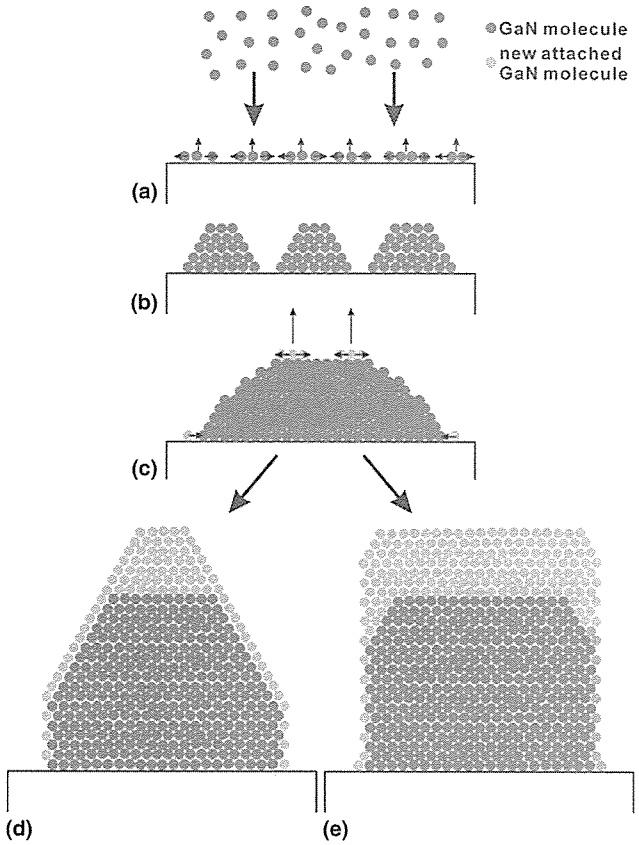

FIG. 6. Schematic illustrations of the growth process of GaN nanorod: (a) initial adsorbed stage, (b) small GaN islands formation, (c) formation of nucleus for GaN nanorod, (d) needle-like nanorod formation, and (e) rod-like nanorod formation.

rod-like shape have made possible the fabrication of the optical devices such as 1D lasers, because their uniform diameter enhances the performance, needle-like GaN nanorods have been excellent candidates for potential applications in field emitters, fine tips for scanning tunneling microscopy and atomic force microscopy, and nanomanipulation tools.[24] The tip morphologies of the GaN nanorods are moderately controlled by changing growth temperature.

IV. SUMMARY AND CONCLUSIONS

Vertically well-aligned GaN nanorods were grown on Al_2O_3 (0001) substrates by HVPE method without a catalyst at different growth temperatures. The tip morphologies and the strain of the GaN nanorods were significantly affected by T_2, T_3, and the temperature difference between T_2 and T_3. The low T_2 and the small degree of the supersaturation due to the temperature difference led the GaN layer to form the 2D thin film instead of the 1D nanorod. The tip diameter of the GaN nanorods was tapered with decreasing temperature difference between T_2 and T_3, or the degree of supersaturation. The magnitudes of the strain and the stress existing in the GaN layer

near the interface were strongly correlated to the growth rate, and the strain of the GaN layer was decreased with increasing growth rate. The formation mechanisms of the GaN nanorods grown on the Al_2O_3 (0001) substrates are described on the basis of the experimental results. These results can help improve understanding of the microstructural properties and the formation mechanisms of the GaN nanorods grown on Al_2O_3 (0001) substrates by using HVPE without a catalyst.

ACKNOWLEDGMENTS

This work was supported by the Korea Science and Engineering Foundation (KOSEF) grant funded by the Korea government (MEST) (No. R0A-2007-000-20044-0) and also by the Korea Science and Engineering Foundation through the Quantum Functional Semiconductor Research Center at Dongguk University.

REFERENCES

1. H. Yoshida, Y. Yamashita, M. Kuwabara, and H. Kan: A 342-nm ultraviolet AlGaN multiple-quantum-well laser diode. *Nat. Photonics* **2,** 551 (2008).
2. C. Lu, X. Xie, X. Zhu, D. Wang, A. Khan, I. Diagne, and S.N. Mohammad: High-temperature electrical transport in $Al_xGa_{1-x}N$/GaN modulation doped field-effect transistors. *J. Appl. Phys.* **100,** 113729 (2006).
3. K. Lee, Z. Wu, Z. Chen, F. Ren, S.J. Pearton, and A.G. Rinzler: Single wall carbon nanotubes for *p*-type ohmic contacts to GaN light-emitting diodes. *Nano Lett.* **4,** 911 (2004).
4. A.T. Schremer, J.A. Smart, Y. Wang, O. Ambacher, N.C. MacDonald, and J.R. Shealy: High electron mobility AlGaN/GaN heterostructure on (111) Si. *Appl. Phys. Lett.* **76,** 736 (2000).
5. T. Fujii, Y. Gao, R. Sharma, E.L. Hu, S.P. DenBaars, and S. Nakamura: Increase in the extraction efficiency of GaN-based light-emitting diodes via surface roughening. *Appl. Phys. Lett.* **84,** 855 (2004).
6. H.H. Huang, H.Y. Zeng, C.L. Lee, S.C. Lee, and W.I. Lee: Extended microtunnels in GaN prepared by wet chemical etch. *Appl. Phys. Lett.* **89,** 202115 (2006).
7. S. Dhar, L. Pérez, O. Brandt, A. Trampert, K.H. Ploog, J. Keller, and B. Beschoten: Gd-doped GaN: A very dilute ferromagnetic semiconductor with a Curie temperature above 300 K. *Phys. Rev. B* **72,** 245203 (2005).
8. K. Linthicum, T. Gehrke, D. Thomson, E. Carlson, P. Rajagopal, T. Smith, D. Batchelor, and R. Davis: Pendeoepitaxy of gallium nitride thin films. *Appl. Phys. Lett.* **75,** 196 (1999).
9. S. Nakamura, M. Senoh, S. Nagahama, N. Iwasa, T. Yamada, T. Matsushita, H. Kiyoku, Y. Sugimoto, T. Kozaki, H. Umemoto, M. Sano, and K. Chocho: InGaN/GaN/AlGaN-based laser diodes with modulation-doped strained-layer superlattices grown on an epitaxially laterally overgrown GaN substrate. *Appl. Phys. Lett.* **72,** 211 (1998).
10. J.C. Johnson, H.J. Choi, K.P. Knutsen, R.D. Schaller, P. Yang, and R.J. Saykally: Single gallium nitride nanowire lasers. *Nat. Mater.* **1,** 106 (2002).
11. A.M. Morales and C.M. Lieber: A laser ablation method for the synthesis of crystalline semiconductor nanowires. *Science* **279,** 208 (1998).
12. M. Law, J. Goldberger, and P. Yang: Semiconductor nanowires and nanotubes. *Annu. Rev. Mater. Res.* **34,** 83 (2004).
13. Y. Xia, P. Yang, Y. Sun, Y. Wu, B. Mayers, B. Gates, Y. Yin, F. Kim, and H. Yan: One-dimensional nanostructures: Synthesis, characterization, and applications. *Adv. Mater.* **15,** 353 (2003).
14. J.G. Lu, P. Chang, and Z. Fan: Quasi-one-dimensional metal oxide materials—Synthesis, properties and applications. *Mater. Sci. Eng., R* **52,** 49 (2006).
15. T. Kuykendall, P. Pauzauskie, S. Lee, Y. Zhang, J. Goldberger, and P. Yang: Metalorganic chemical vapor deposition route to GaN nanowires with triangular cross sections. *Nano Lett.* **3,** 1063 (2003).
16. H.Y. Chen, H.W. Lin, C.H. Shen, and S. Gwo: Structure and photoluminescence properties of epitaxially oriented GaN nanorods grown on Si (111) by plasma-assisted molecular-beam epitaxy. *Appl. Phys. Lett.* **89,** 243105 (2006).
17. H.M. Kim, D.S. Kim, D.Y. Kim, T.W. Kang, Y.H. Cho, and K.S. Chung: Growth and characterization of single-crystal GaN nanorods by hydride vapor-phase epitaxy. *Appl. Phys. Lett.* **81,** 2193 (2002).
18. G. Seryogin, I. Shalish, W. Moberlychan, and V. Narayanamurti: Catalytic hydride vapour phase epitaxy growth of GaN nanowires. *Nanotechnology* **16,** 2342 (2005).
19. K.H. Lee, Y.H. Kwon, S.Y. Ryu, T.W. Kang, J.H. Jung, D.U. Lee, and T.W. Kim: Microstructural properties and atomic arrangements of GaN nanorods grown on Si (111) substrates by using hydride vapor-phase epitaxy. *J. Cryst. Growth* **310,** 2977 (2008).
20. E. Aujol, J. Napierala, A. Trassoudaine, E. Gil-Lafon, and R. Cadoret: Thermodynamical and kinetic study of the GaN growth by HVPE under nitrogen. *J. Cryst. Growth* **222,** 538 (2001).
21. K.H. Lee, J.Y. Lee, H.C. Jeon, T.W. Kang, H.Y. Kwon, and T.W. Kim: Initial formation mechanisms of $(Ga_{1-x}Mn_x)N$ nanorods grown on Al_2O_3 (0001) substrates. *J. Mater. Res.* **23,** 3275 (2008).
22. V.S. Harutyunyan, A.P. Aivazyan, E.R. Weber, Y. Kim, Y. Park, and S.G. Subramanya: High-resolution x-ray diffraction strain–stress analysis of GaN/sapphire heterostructures. *J. Phys. D: Appl. Phys.* **34,** A35 (2001).
23. R.K. Debnath, R. Meijers, T. Richter, T. Stoica, R. Calarco, and H. Lüth: Mechanism of molecular-beam-epitaxy growth of GaN nanowires on Si (111). *Appl. Phys. Lett.* **90,** 123117 (2007).
24. G. Hashiguchi, T. Goda, M. Hosogi, K. Hirano, N. Kaji, Y. Baba, K. Kakushima, and H. Fujita: DNA manipulation and retrieval from an aqueous solution with micromachined nanotweezers. *Anal. Chem.* **75,** 4347 (2003).